Applied Ocean Research 69 (2017) 1–9

Contents lists available at ScienceDirect

Applied Ocean Research

journal homepage: www.elsevier.com/locate/apor

Efficient processing of water wave records via compressive sensing and joint time-frequency analysis via harmonic wavelets

Valentina Laface [a], Ioannis A. Kougioumtzoglou [b], Giovanni Malara [a], Felice Arena [a,*]

[a] Natural Ocean Engineering Laboratory (NOEL), "Mediterranea" University of Reggio Calabria, Loc. Feo di Vito, 89122 Reggio Calabria, Italy
[b] Department of Civil Engineering & Engineering Mechanics, Columbia University, New York, NY 10027, USA

ARTICLE INFO

Article history:
Received 4 June 2017
Received in revised form
22 September 2017
Accepted 27 September 2017

Keywords:
Wave data
Compressive sensing
Evolutionary power spectrum
Non-stationary stochastic process
Harmonic wavelets

ABSTRACT

A methodology is proposed for efficient processing of sea wave field data via compressive sensing (CS), and joint time-frequency analysis via harmonic wavelets (HWs) based evolutionary power spectrum (EPS) estimation. In this regard, it is possible to record and store relatively long wave data sequences, whereas the commonly adopted in-practice assumption of stationary data is abandoned. Currently, most wave records are measured by buoys, which acquire data for a time interval representative of stationary time series. Next, following a Fourier transform processing, only few spectral parameters are stored. Thus, detailed information about localized-in-time phenomena are completely lost. Herein, it is shown that CS can be adopted for efficiently compressing and reconstructing wave data, while retaining localized information. For this purpose, CS is used in conjunction with a HW basis for processing long time series. In particular, storage capacity demands are drastically decreased as only the HW coefficients need to be saved. These are determined from a randomly-sampled record by invoking a $L_{1/2}$ norm minimization procedure. The resulting reconstructed record, being longer than conventional wave time series, can no longer be regarded as stationary; thus, a HW based EPS estimate is employed for describing the joint time-frequency features of the record. Finally, the reliability of the methodology is assessed by analyzing wave field data measured at the Natural Ocean Engineering Laboratory (NOEL) of Reggio Calabria. Specifically, comparisons between original and reconstructed records demonstrate a satisfactory agreement regarding the time-histories, and the estimated EPS and relevant statistical quantities, even for up to 60% missing/removed data.

1. Introduction

The concept of sea state has been instrumental in marine engineering, as it has facilitated the development of most modern analysis techniques within the context, for instance, of wave statistics, structural reliability, and mechanics of extreme waves. The primary assumption behind this concept relates to the fact that the free surface displacement recorded during a certain time interval (of order of 100–200 waves) can be construed as part of a realization of a stochastic process with given probability density function (pdf) and power spectral density (psd) [1]. In this context, although Gaussian processes have certainly been the most utilized for determining sea wave statistics, non-Gaussian models are also quite established for describing non-linear phenomena [2,3].

Nevertheless, the underlying assumption of stationarity has never really been questioned by the majority of researchers. In this regard, some observations were noted by Liu et al. [4,5]. Specifically, they observed that conventional approaches used for describing the wave growing process are limited in the sense that they are unable to describe time-localized mechanisms such as wave grouping or wave breaking. This inadequacy of the approaches also relates to the fact that conventional observation intervals are limited to 20–30 min windows, a widely utilized sea state duration [6]. Extending the recording time window is certainly attractive because of the possibility of acquiring more information about the recorded physical processes. However, this extension must cope with additional challenges. First, new tools are necessary for processing longer data sequences due to the increased storage capacity demands, and second, the measured extended signal may exhibit time-varying statistics, and thus, cannot be construed as a realization compatible with an underlying stationary stochastic process.

To address the above challenges, this paper employs and assesses the capabilities of two potent tools/concepts for treating

* Corresponding author.
E-mail addresses: valentina.laface@unirc.it (V. Laface), ikougioum@columbia.edu (I.A. Kougioumtzoglou), giovanni.malara@unirc.it (G. Malara), arena@unirc.it (F. Arena).

https://doi.org/10.1016/j.apor.2017.09.011
0141-1187/

long, non-stationary, free surface data sequences; that is, compressive sensing (CS), and evolutionary power spectrum (EPS).

Compressive sensing circumvents the limitation posed by the Nyquist-Shannon sampling rate theorem [7,8] and can be used for acquiring/sampling and storing longer free surface time histories. Currently, wave data are recorded mainly by buoys equipped with accelerometers, which measure the acceleration and provide the free surface displacement by numerical integration [9]. Typically, data are recorded with a sampling interval that varies between 0.5 and 1 s (depending on wave characteristics at the considered site) for a duration of 20–30 min, whereas the time interval between successive records may vary from half an hour to three hours. Next, the Fourier transform is applied on each record of sea surface elevation, and only spectral data including significant wave height H_s and peak spectral period T_p are provided to the final users. The choice of the record duration relates to the definition of sea state. In this regard, it is long enough to be representative of the sea state conditions, but short enough at the same time to guarantee stationarity of the process. Further, the time interval between successive records is chosen to be short enough to capture adequately the long-term variability of the sea conditions. Obviously, this procedure is theoretically consistent with the sea state concept, but it is also dictated by the need for limiting the amount of stored data, and ultimately, lowering the equipment cost.

However, if only synthetic parameters are stored, information about local phenomena, such as freak waves, is completely lost [10]: for this reason, storing full data records is desirable. In this context, considering that sea waves are characterized by a relatively small number of dominant frequencies when expanded in the frequency domain, the CS approach [11,12] can be applied to reconstructing signals that contain sampling gaps (either deliberately for storage capacity purposes or due to equipment failure) in the time domain by selecting an appropriate basis [13–16].

Further, EPS were introduced for describing the time-varying frequency content of non-stationary stochastic processes [17]. The problem of treating non-stationary signals was initially addressed by the short time Fourier transform [18–20] and, later, by the wavelet transform (WT) [21,22] among other alternatives. In this regard, Newland [23–25] introduced the family of generalized harmonic wavelets (GHWs), which was employed in Spanos et al. [26] to estimate the EPS of non-stationary stochastic processes from available realizations. Thus, a GHW-based EPS estimation technique was developed. Further, GHWs have proven to be efficacious for structural dynamics-related applications due to their non-overlapping, box-shaped frequency spectra, their orthogonality properties, and the convenience of combining harmonic balance with statistical linearization techniques [27,28]. Applications of wavelets to ocean engineering related problems are increasing considerably, due to their versatility. For instance, the work of Massel [29] demonstrated the capability of the wavelet transform to provide a time-frequency representation of wave signals. Other contributions relate to studies on wave breaking [30], occurrence of abnormal waves [31] and time series forecasting [32,33].

In the ensuing sections, it is demonstrated that a) GHWs can be used in conjunction with the concept of EPS for processing and capturing time-varying features of free surface elevation records, and b) CS can be combined with a GHW basis for compressing free surface records. Finally, the theoretical developments are exemplified by analyzing long experimental free surface displacement data.

2. Processing and analysis of non-stationary time series

In this section the key elements related to the implementation of the EPS estimation and the CS based reconstruction are delineated. These two tools are strictly connected to each other in the ensuing implementation via the representation adopted for the time series analyses. Indeed, the EPS estimation is pursued via the GHWT, which is invoked also during the signal reconstruction. Other representations can be utilized, as well. However, this one is adopted because it ensures non-overlapping intervals at different scales along the frequency axis, and thus, desirable orthogonality properties hold true.

2.1. Evolutionary power spectrum estimation via the GHWT

The wavelet transform of a finite energy stochastic process $f(t)$ provides a time-frequency representation of $f(t)$. Its calculation relates to the determination of a series of wavelet coefficients at different scales j and time positions k. Note that the scale parameter is related to the frequency, whereas the general form of a continuous wavelet transform of a stochastic process $f(t)$ is given by

$$[W_\Psi f](j,k) = \frac{1}{|j|^{1/2}} \int_{-\infty}^{+\infty} f(t) \Psi^* \left(\frac{t-k}{j} \right) \mathrm{d}t. \tag{1}$$

In Eq. (1) $[W_\Psi f](j,k)$ is the wavelet coefficient at scale j and time position k, the function $\psi(t)$ is the mother wavelet and the symbol $(^*)$ denotes the complex conjugate of $\psi(t)$. Eq. (1) represents a convolution operation between $f(t)$ and the basis functions obtained by properly scaling and translating the mother wavelet. The wavelet coefficients provide a measure of the similarity between $f(t)$ and the wavelet. Thus, the higher the correlation is, the larger the coefficient will be.

Focusing on the specific family of harmonic wavelets, they are defined to have a band limited spectrum, whereas two indices (m,n) are used to define the frequency bands and to control their frequency content. Herein, the generalized harmonic wavelet is considered, which is expressed in the frequency domain as [24]:

$$\Psi_{(m,n),k}(\omega) = \begin{cases} \dfrac{1}{(n-m)\Delta\omega} e^{-\dfrac{i\omega k T_0}{n-m}}; & \text{for } m\Delta\omega \le \omega < n\Delta\omega \\ 0; & \text{elsewhere} \end{cases} \tag{2}$$

where T_0 is the total time duration of the signal under consideration, m and n are integer numbers defining the frequency band $(n>m)$, and $\Delta\omega = 2\pi/T_0$. The complex harmonic wavelet coefficients are given by:

$$[W^G_{(m,n),k} f(t)] = \frac{(n-m)}{T_0} \int_{-\infty}^{+\infty} f(t) \Psi^*_{(m,n),k}(t)\, \mathrm{d}t, \tag{3}$$

and the evolutionary power spectrum can be estimated as [26]

$$S_f(\omega,t) = S^f_{(m,n),k} = \frac{E(|[W^G_{(m,n),k} f(t)]^2|)}{(n-m)\Delta\omega};$$

$$\text{with} \quad \begin{cases} m\Delta\omega \le \omega < n\Delta\omega, \\ \dfrac{kT_0}{(n-m)} \le t < \dfrac{(k+1)T_0}{(n-m)}. \end{cases} \tag{4}$$

The estimation of the EPS of a non-stationary stochastic process $f(t)$ via Eq. (4) requires the calculation of the wavelet coefficient by means of Eq. (3) based on an available ensemble of process realizations. From a practical point of view it is worth noting that the GHWT can be numerically determined by utilizing the Fast Fourier Transform (FFT), which offers significant computational advantages [34].

2.2. Compressive sensing

Compressive sensing [35,12] is a recently developed technique widely utilized in signal and image processing subject to vastly under-sampled data. Further, it has proven to be a potent technique for data reconstruction when recorded signals exhibit gaps or missing data in the time domain [13]. This framework provides the potential to circumvent the standard sampling theorem that states that a time signal can be fully determined only if sampled at time intervals smaller or equal to half its maximum frequency [7,8]. In this regard, under certain assumptions, CS allows for signal reconstruction even if the maximum frequency is greater than half the sampling rate [36]. The technique essentially relates to expanding the time recorded signal in a known basis, and solving an undetermined linear system of equations via an L_p –norm $(0 < p \leq 1)$ minimization procedure for obtaining the sparsest representation of the signal in the selected basis. In general, the resulting system of equations takes the form

$$y = Ax, \tag{5}$$

where y is the sample record with missing data, A is the so-called sampling matrix and x is the vector of the expansion coefficients. Vectors x and y have dimension N_0 and N_0-N_m respectively, N_0 being the original signal length and N_m is the number of missing data, while A is a $(N_0$-$N_m)$ by N_0 matrix.

The technique requires that both the signal and the sampling matrix satisfy certain properties [37]. Specifically, the signal must be sparse in the selected basis. That is, it can be represented by a number of coefficients smaller than that determined at the Shannon-Nyquist rate. Further, the sampling and transformation domains must have high incoherence, which implies a non-sparse representation of the signal in the sampling domain. In addition to signal sparsity and incoherence, the sampling matrix must satisfy the restricted isometry property (RIP) which implies that if the signal has sparsity K (i.e. it can be represented by K non-zero coefficients) any matrix obtained by K randomly selected columns of A should have full rank and be nearly orthonormal.

Irrespective of the specific basis chosen, the implementation of CS consists of the following two main steps:

1. Construction of the sampling matrix A;
2. L_p-norm $(0 < p \leq 1)$ minimization for determining the sparsest representation of the signal.

Herein, the case of non-stationary signals is considered for which GHWs are inherently well-suited as a basis due to their joint time-frequency resolution capabilities; see also Comerford et al. [13–15] and Zhang et al. [16]. The sampling matrix A is obtained by firstly generating a N_0 by N_0 matrix. Then, N_m rows corresponding to the position of the missing data are removed. The GHW basis are generated by inverse FFT following the procedure shown in Fig. 1. A single GHW is shifted $(n–m)$ times in the time domain to form an orthogonal basis. Then, once the construction of A is completed, the rows corresponding to the missing data are removed and Eq. (5) is solved via L_p-norm $(0 < p \leq 1)$ minimization and the sparsest solution for x is determined. Finally, the signal is reconstructed by multiplying the original sampling matrix A by the expansion coefficients x.

3. Field data analysis

In this section, a long non-stationary record of free surface elevation is considered. The first objective of the analysis relates to proposing a way for sampling sea surface elevation data without the constraint of stationarity. Related to this is the objective of storing many more data than those acquired by the conventional approach involving an FFT data analysis and storage of synthetic spectral parameters (e.g. H_s and T_p) [38]. The constraint of stationarity implies record durations between 20 and 30 min. By removing it, the record duration can be increased from few tens of minutes to the order of hours. In this manner, the signal under consideration can no longer be regarded as stationary, and thus, resorting to the concept of EPS is necessary. Obviously, an increased duration implies many more data in a given record. To overcome the problem of storing an excessive number of data points, a CS technique is applied for compressing data via expanding them in a certain basis in which the signal is sparse. Thus, the signal can be readily reconstructed by employing a very small number of non-zero coefficients. The main idea is to record all the data for the given duration and then to remove randomly a certain fraction of them and produce a signal with time gaps. The new “incomplete” signal is then expanded by the CS technique and only the values and the position of the non-zero expansion coefficients are stored and used for recovering the original signal when time-domain analyses are to be performed.

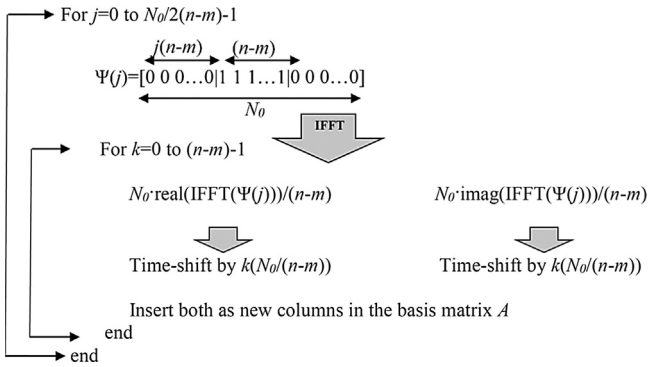

Fig. 1. Flowchart of the algorithm for constructing the sampling matrix with HW basis.

The analysis utilizes a set of sea surface elevation records measured at Natural Ocean Engineering Laboratory (NOEL) of Reggio Calabria (Italy). In particular, the first one has a total duration of 2500 s sampled at 10 Hz and has been recorded during the peak stage of a sea storm occurred in September 2014. This particular record is chosen because it is associated with severe wave conditions characterized by the occurrence of quite large waves. In addition, five short records of a duration of about ten minutes, recorded during different wave conditions, are processed to investigate the effectiveness of the methodology in a variety of sea states and to demonstrate the general validity of the results.

Note that at NOEL location the significant wave height ranges between 0.2 and 1.2 m, with peak spectral periods between 2 and 3.6 s. The peculiarity of the lab is that local wind from NNW often generates sea states consisting of pure wind waves that represent a small scale model (1:5–1:20), in Froude similarity, of ocean storms (see www.noel.unirc.it).

3.1. Compression and reconstruction of free surface elevation data

The compression of sea surface elevation data is performed via the CS technique using the GHW basis and following the procedure described in Section 2.2. For this purpose, $L_{1/2}$ norm minimization is considered due to its ability to promote solutions sparser than the ones typically obtained by alternative L_1 norm minimization approaches [16]. In this context, the problem is recast in the form

$$\min |x|_{L_{1/2}} \quad \text{subject to} \quad y = Ax. \tag{6}$$

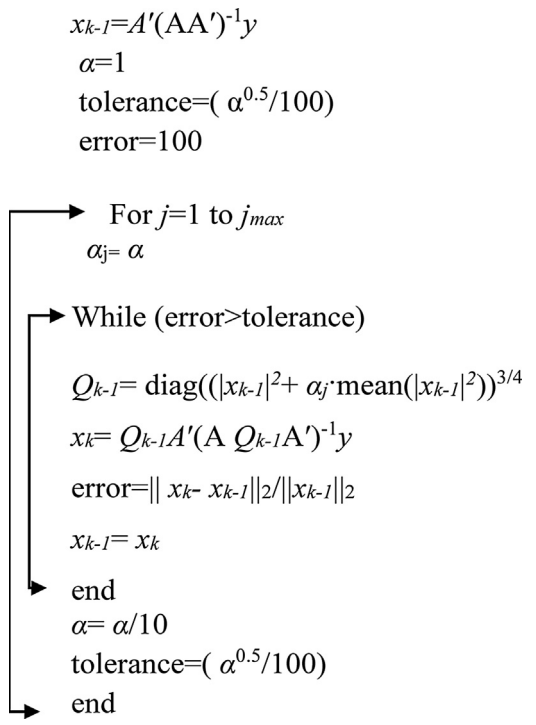

Fig. 2. Flowchart for implementing the algorithm minimizing the $L_{1/2}$ norm.

Next, to solve the minimization problem (6), the Lagrangian $L(x, \lambda)$ is introduced. Specifically,

$$L(x,\lambda)=\sum_i |x_i|^{1/2}+\lambda^T(Ax-y), \tag{7}$$

whereas the following equation is obtained by setting the partial derivatives of Eq. (7) with respect to x and λ equal to zero:

$$x=QA'(AQB')^{-1}y, \tag{8}$$

where $Q=diag(|x|^{\frac{2}{3}})$.

Eq. (8) may be solved by an iterative procedure involving updated values of Q determined from the solution of each previous iteration as

$$x_k=Q_{k-1}A'(AQ_{k-1}B')^{-1}x, \tag{9}$$

with

$$Q_{k-1}=diag(|x_{k-1}|^{\frac{2}{3}}). \tag{10}$$

Further, to avoid division by zero as the algorithm converges, a decreasing parameter α is introduced for regularizing the optimization procedure. That is,

$$Q_{k-1}=diag(|x_{k-1}|^2+\alpha_j mean(|x_{k-1}|^2))^{\frac{3}{4}}, \tag{11}$$

$$\alpha_j=\frac{\alpha_{j-1}}{10}, \tag{12}$$

where $\alpha_0=1$ and for each α_j Eq. (9) is evaluated until the following condition is satisfied:

$$\frac{\|x_k-x_{k-1}\|_2}{\|x_{k-1}\|_2}<\frac{\sqrt{\alpha_j}}{100}. \tag{13}$$

The iterative procedure delineated above (see Fig. 2) is implemented for determining the sparsest solution for the expansion coefficients vector x. Next, the variability of the error between the original and the reconstructed signals with increasing percentage of missing/removed data is investigated. For each record, ten different positions of missing data are randomly generated. Results

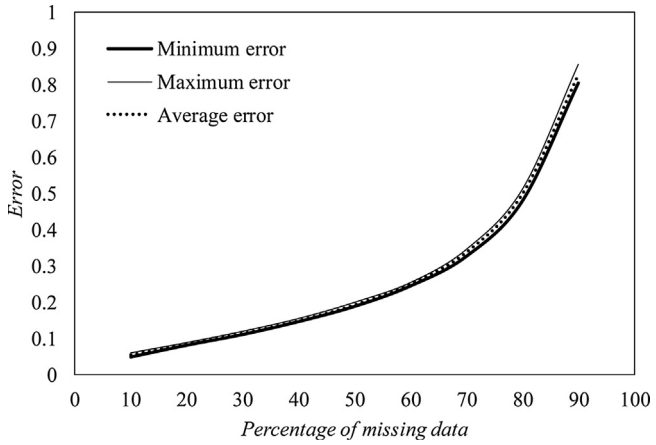

Fig. 3. Maximum, minimum and average error with for different percentage of missing data, obtained considering ten different random positions of the missing data.

are shown in Fig. 3, where minimum, maximum and average (calculated from the 10 configurations) errors are represented as a function of percentage of missing data. For the calculation, the following definition of the error is considered:

$$error=\frac{\|y_{original}-y_{reconstructed}\|_2}{\|y_{original}\|_2}, \tag{14}$$

where $y_{original}$ is the original free surface record and $y_{reconstructed}$ is the one reconstructed by CS. It is seen that the error is almost insensitive to the missing data positions, while it increases as the percentage of missing data increases. Specifically, it is below 0.3 for up to 60% missing data, below 0.5 for missing data percentage between 60% and 80%, and then it increases rapidly for higher percentage of missing data. Fig. 4 shows the comparison between original and reconstructed signals with 20%, 40% and 60% missing data for a time window of 50 s. The figure shows that no significant differences in the reconstructed signals are detected for missing data between 20% and 40%, while from 40% to 60% the differences are limited. Fig. 5 shows a similar comparison. In this case, the figure shows the maximum recorded crest height and highlights the fact that the technique also allows reconstruction of the extreme waves. Fig. 6 shows the expansion coefficients x_i estimated from the record with 40% of missing data. It is seen that the majority of the coefficients are close to zero. Therefore, the small number of the non-zero elements reduces drastically the required memory for storage in comparison with treating the original "complete" signal. Further analysis is conducted for quantifying the percentage of coefficients that can be neglected and replaced by zeros without compromising essentially the quality of the reconstruction. Fig. 7 shows the result obtained for the signal with 40% missing data as a function of the percentage of neglected coefficients. The figure emphasizes the fact that neglecting up to 80% of the coefficients the error is lower than 0.1 and increases rapidly for percentages greater than 90%. Thus, from a practical point of view, this suggests that all the coefficients lower than a given threshold (in absolute value) can be replaced by zeros. Following such an approach, it is possible to store approximately only 20% of coefficients x_i, without losing any crucial information about the signal.

Further analysis is conducted by processing five sea states characterized by different H_s–T_p pairs. In addition, for each sea state the parameter of the spectrum Ψ^*, indicative of how much narrow-band the spectrum is and defined as the ratio between the absolute minimum and the absolute maximum of the auto-covariance function of the free surface elevation, is calculated for inferring the nature of the recorded sea state [6]. For instance, $\Psi^*=0.73$ relates to a JONSWAP spectrum [39], $\Psi^*=0.63$ relates to a

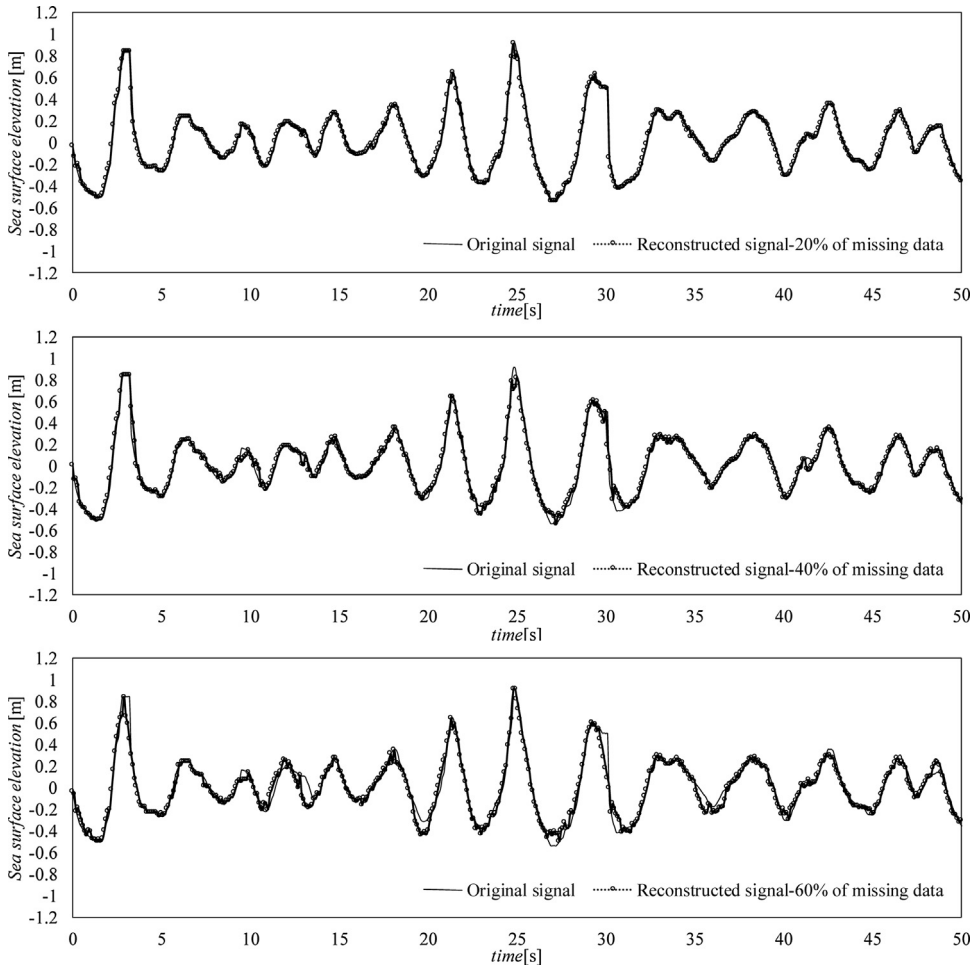

Fig. 4. Comparison between original signal (no missing data) and reconstructed signal for a portion of the record of 50 s.

Table 1
Sea state characteristics and errors pertaining to various fractions of missing data.

			Fraction of missing data			
H_s [m]	T_p [s]	Ψ^*	20%	40%	60%	80%
0.52	3.41	0.62	0.063	0.113	0.214	0.482
0.16	2.74	0.42	0.073	0.140	0.244	0.570
0.18	5.71	0.37	0.055	0.095	0.168	0.428
0.20	6.32	0.47	0.065	0.117	0.203	0.473
0.35	2.94	0.71	0.062	0.111	0.230	0.513

Pierson and Moskowitz [40] spectrum, while smaller values of the parameter are representative of mixed sea states. Finally, for each record the error (14) is estimated by considering various fractions of missing/removed data. The results are summarized in Table 1 in conjunction with the sea states characteristics. It is seen that although the accuracy of the reconstruction depends on the fraction of missing data, it appears rather insensitive to nature of the wave record. In this regard, it is observed that, for a specified record, the error of the reconstruction increases as the percentage of the missing data grows. The results are in agreement with the ones of Fig. 3, which shows that the error is lower than 0.3 for percentages of missing data up to 60% and less than 0.6 for percentages up to 80%. Considering the low correlation between results and the nature of the record, the successive analyses focus on the first nonstationary record pertaining to the storm peak.

3.2. EPS estimation of original and reconstructed sea surface elevation record

In this sub-section, the EPS of original and reconstructed signals with 20%, 40% and 60% missing data are estimated and compared. Results are shown in Fig. 8. The Figure shows that the EPS peaks are underestimated as the percentage of missing data increases. Further, the EPSs of both original and reconstructed signals show several peaks in the time domain that describe the evolution of the sea condition in time during the whole sea surface record. For each EPS the highest peak occurs at the very beginning of the record. This relates to the fact that the first half of the record pertains to a storm peak stage, during which the energy content is larger. The EPS estimated from the reconstructed and original signals at given time instants are compared in Fig. 9. The first plot ($t = 240$ s) pertains to the time instant of the peak of EPS, while the others are selected every 480 s. Thus, covering the entire duration of the record. Results exhibit a very good agreement between original and reconstructed EPSs at each considered time instant, even in the cases of 40% and 60% missing data.

Finally, it is emphasized that the EPS provides information consistent with the classical approach of the sea state theory. Indeed, the peak frequency ω_p and the zero order moment m_0 of the spectrum at a fixed time instant are quite similar to the ones obtained by processing short time records of the wave data via FFT. Fig. 10 shows a direct comparison between them, where the corresponding "stationary" quantities are calculated by processing only 5 min

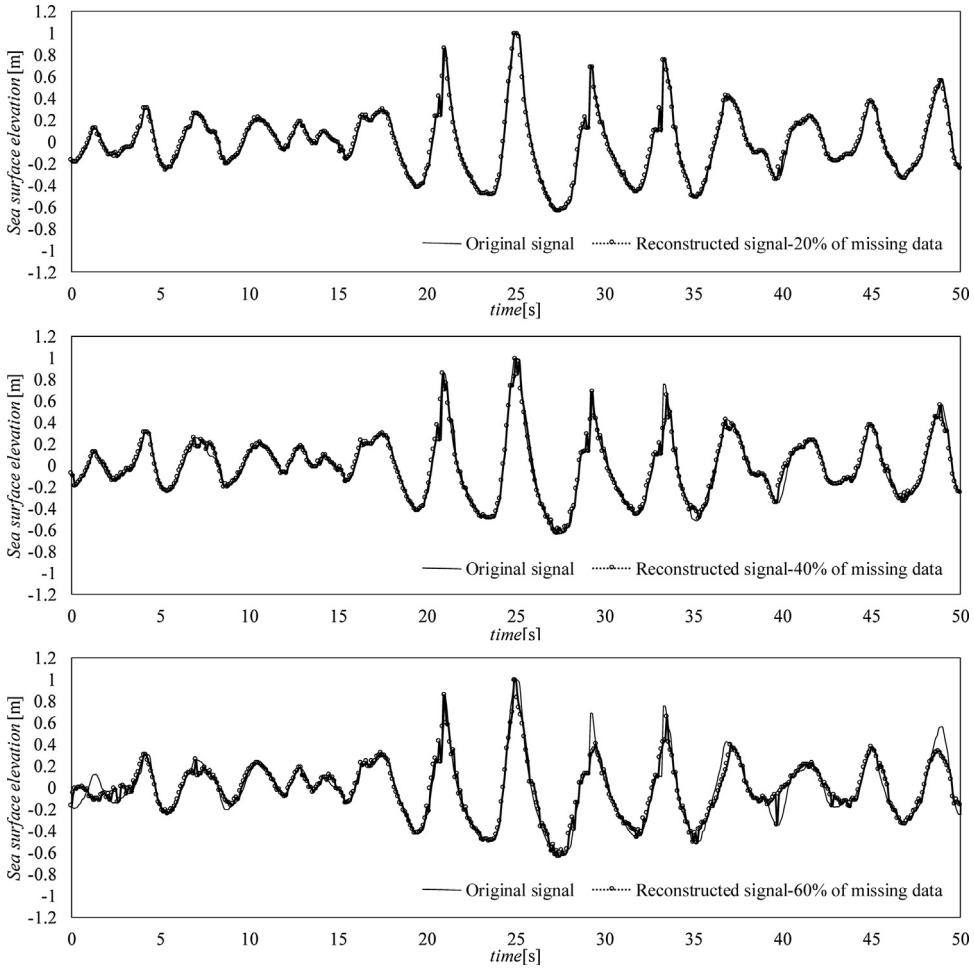

Fig. 5. Comparison between original signal (no missing data) and reconstructed signal for a portion of the record of 50 s. Record pertaining to the maximum recorded crest height.

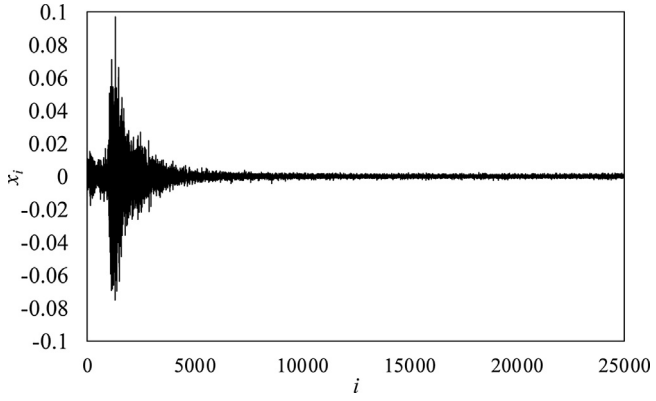

Fig. 6. Expansion coefficients x_i estimated from the record with 40% missing data.

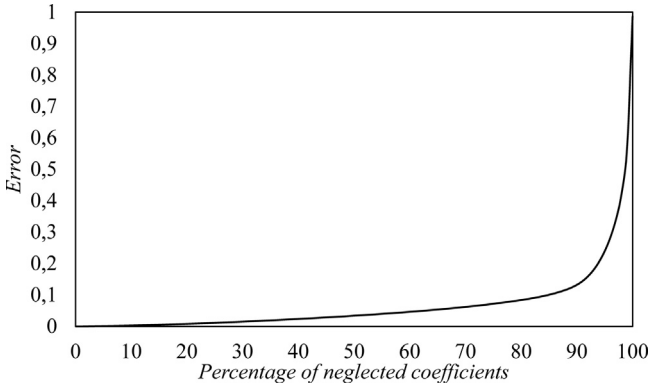

Fig. 7. Error between a reconstructed free surface and a reconstructed free surface obtained by neglecting a certain percentage of expansion coefficients.

of data centered at the selected time instants. It is shown that these key quantities agree reasonably well to each other.

3.3. Comparison between cumulative distribution functions of wave height H of original and reconstructed signals

The previous comparisons highlighted the fact that there are discrepancies between the original and reconstructed signals. Therefore, it is deemed necessary to examine to what extent the reconstructed signal can be used for pursuing typical statistical analyses relevant to marine applications. This problem is addressed here by computing the cumulative distribution function of the crest-to-trough wave height $P(H)$. Specifically, $P(H)$ is computed for both original and reconstructed signals with 20%, 40%, 60% missing data. The numerical results are shown in the semi-logarithmic plot in Fig. 11.

The vertical axis shows the quantity $[1 - P(H)]$, while the horizontal axis is the wave height threshold H. The results show a quite good agreement between $P(H)$ of original and reconstructed signals, especially for 20% and 40% missing data, while a slight deviation is observed for 60% missing data.

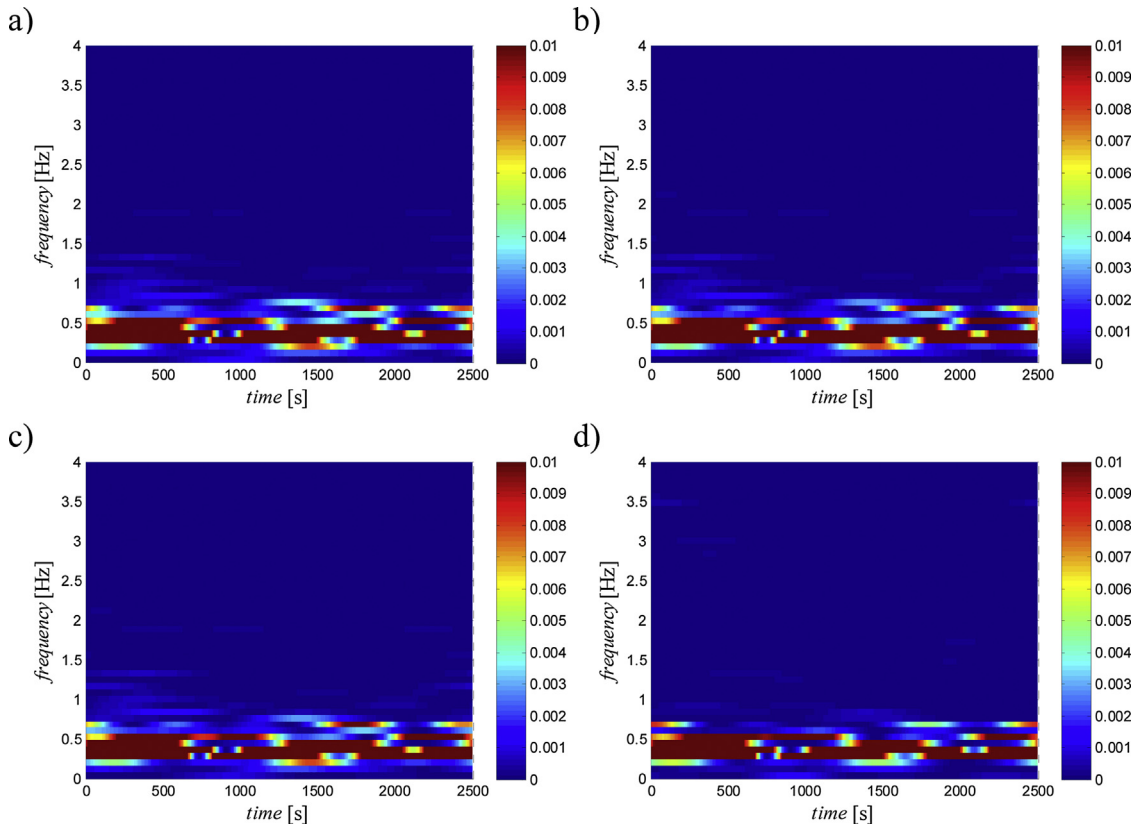

Fig. 8. Comparison between EPSs of a) original signal (no missing data), reconstructed signal with b) 20%, c) 40%, d) 60% missing data. The unit of the EPS is m^2 s/rad.

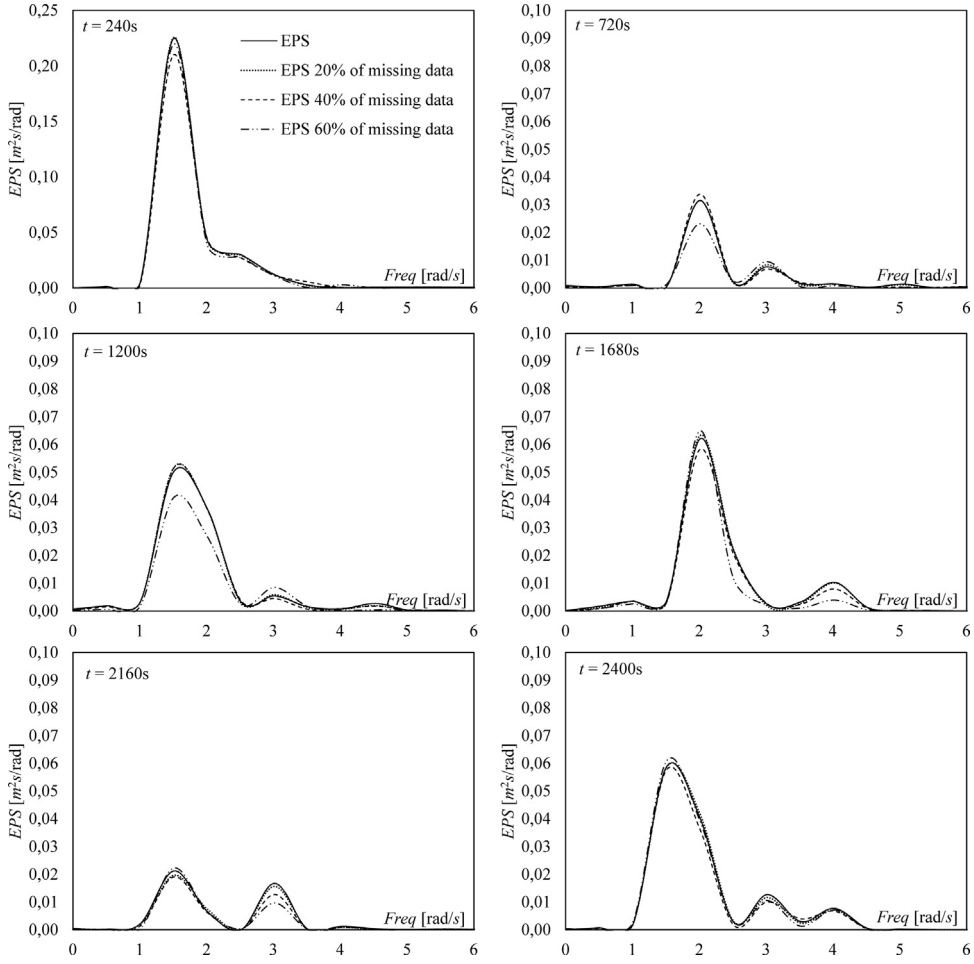

Fig. 9. Comparison between EPSs at given time instants (t = 240 s corresponds to the peak of the EPS calculated starting from the original signal).

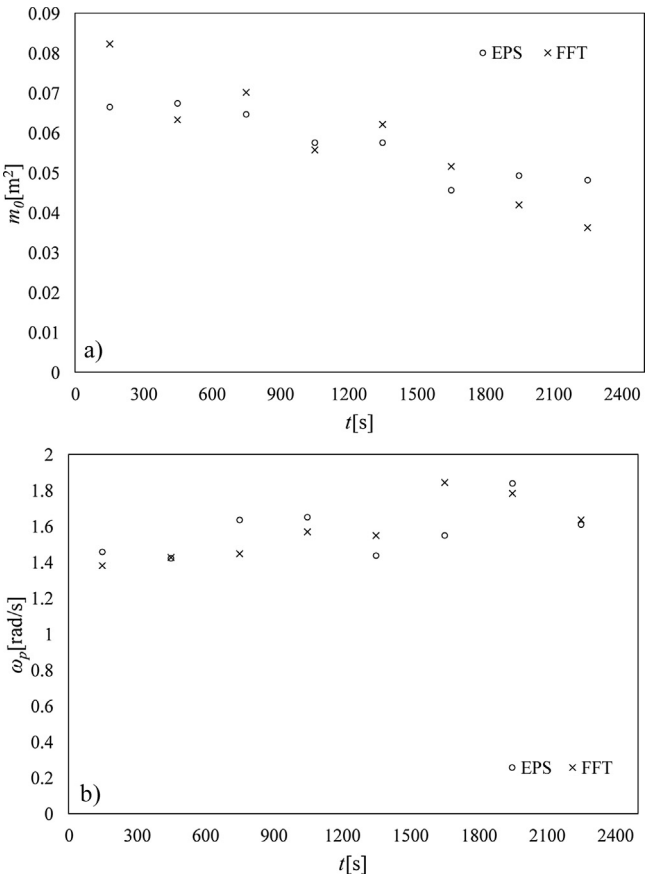

Fig. 10. Comparison between a) the zero order moment m_0 of the spectrum and b) the peak frequency ω_p estimated by GHW and FFT spectrum.

4. Concluding remarks

This paper has focused on the field data analysis of a non-stationary free surface elevation record by employing the Evolutionary Power Spectrum (EPS) concept, and Compressive Sensing (CS) techniques in conjunction with a Generalized Harmonic Wavelets (GHW) basis. Specifically, the proposed analysis aimed at assessing the efficiency and reliability of these methods for storing, reconstructing and analyzing/interpreting water wave data.

It has been shown that CS in conjunction with a GHW basis has been efficacious in treating relatively long records by processing only a small fraction of randomly selected data points and storing a very small number of coefficients. These coefficients are used then for reconstructing the original record. This feature enables the utilization of significantly less computer memory and, at the same time, storing information about the entire record instead of few synthetic spectral parameters only. In this regard, it has been shown that by retaining only approximately 20% of the GHW coefficients, an excellent signal reconstruction is still possible. The analysis has involved the reconstruction of the original record and the estimation of the associated EPS starting from the original/target with a given percentage of removed data. The comparisons between the original and reconstructed signals, as well as the corresponding EPS, have shown that the errors between the original and reconstructed signals are negligible for up to 40% removed data and are relatively small for up to 60% removed data. Further, it is seen that the accuracy of the reconstruction appears rather insensitive to the nature of the wave record and is quite satisfactory also in the vicinity of very large waves.

Additional analysis has been conducted on the cumulative distribution function of the crest-to-trough wave heights. It has been shown that these are satisfactorily estimated for removed data up to 40%. These analyses suggest that the methods can be applied to field data by considering a percentage of missing/removed data lower or equal to 60%.

Acknowledgements

This paper was developed during the Marie Curie IRSES project “Large Multi- Purpose Platforms for Exploiting Renewable Energy in Open Seas (PLENOSE)” funded by the European Union (Grant Agreement Number: PIRSES-GA-2013-612581).

G. Malara is grateful to ENEA (Agenzia nazionale per le nuove tecnologie, l’energia e lo sviluppo economico sostenibile) for fund-

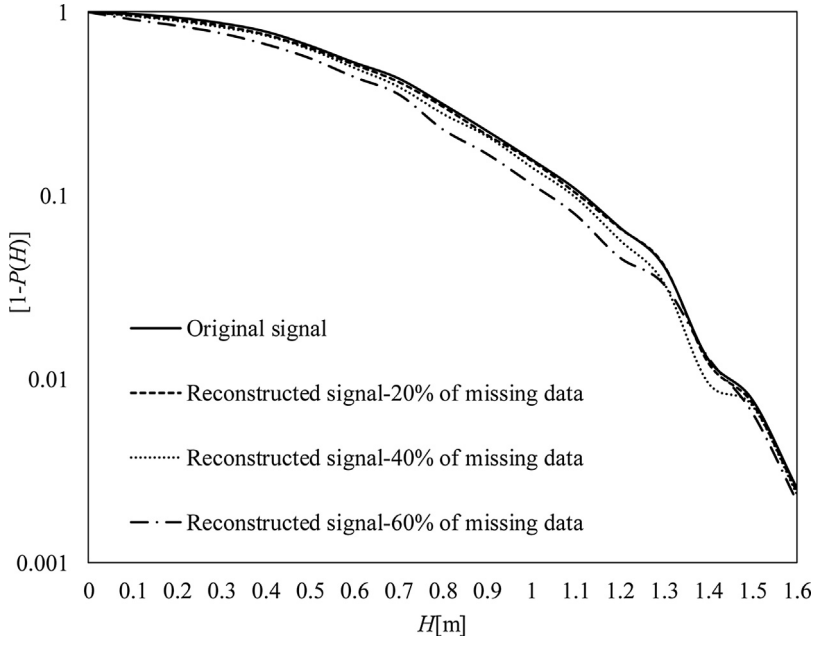

Fig. 11. Comparison between cumulative distribution functions of wave height H calculated from data of the original and reconstructed signals.

ing his activity by the postdoctoral fellowship “Experimental and full scale analysis of wave energy devices”.

I.A. Kougioumtzoglou gratefully acknowledges the support by the CMMI Division of the National Science Foundation, USA (Award number: 1724930).

References

[1] M.K. Ochi, Ocean Waves: The Stochastic Approach, Cambridge University Press, Cambridge, United Kingdom, 2005.
[2] M.K. Ochi, Non-Gaussian random processes in ocean engineering, Probab. Eng. Mech. 1 (1) (1986) 28–39.
[3] N. Moshchuk, R.A. Ibrahim, Response statistics of ocean structures to non-linear hydrodynamic loading part II: non-Gaussian ocean waves, J. Sound Vib. 191 (1) (1996) 107–128.
[4] P.C. Liu, D.J. Schwab, R.E. Jensen, Has wind–wave modeling reached its limit? Ocean Eng. 29 (1) (2002) 81–98.
[5] P.C. Liu, C.-H. Tsai, H.S. Chen, On the growth of ocean waves, Ocean Eng. 34 (10) (2007) 1472–1480.
[6] P. Boccotti, Chapter 3 - Random Wind-Generated Waves: Basic Concepts, Wave Mechanics and Wave Loads on Marine Structures, Butterworth-Heinemann, Oxford, 2015, pp. 43–61.
[7] H. Nyquist, Certain topics in telegraph transmission theory, Trans. Am. Inst. Electr. Eng. 47 (2) (1928) 617–644.
[8] C. Shannon, Comunication in the presence of noise, Proc. Inst. Radio Eng. 37 (1) (1949) 10–21.
[9] M.-C. Huang, J.-Y. Chen, Wave direction analysis from data buoys, Ocean Eng. 25 (8) (1998) 621–637.
[10] M. Onorato, S. Residori, U. Bortolozzo, A. Montina, F.T. Arecchi, Rogue waves and their generating mechanisms in different physical contexts, Phys. Rep. 528 (2) (2013) 47–89.
[11] E.J. Candes, J.K. Romberg, T. Tao, Stable signal recovery from incomplete and inaccurate measurements, Commun. Pure Appl. Math. 59 (8) (2006) 1207–1223.
[12] D.L. Donoho, Compressed sensing, IEEE Trans. Inf. Theor. 52 (4) (2006) 1289–1306.
[13] L.A. Comerford, M. Beer, I.A. Kougioumtzoglou, Compressive sensing based power spectrum estimation from incomplete records by utilizing an adaptive basis, Proceedings of the IEEE Symposium on Computational Intelligence for Engineering Solutions (CIES) (2014).
[14] L. Comerford, I.A. Kougioumtzoglou, M. Beer, Compressive sensing based stochastic process power spectrum estimation subject to missing data, Probab. Eng. Mech. 44 (2016) 66–76.
[15] L. Comerford, H.A. Jensen, F. Mayorga, M. Beer, I.A. Kougioumtzoglou, Compressive sensing with an adaptive wavelet basis for structural system response and reliability analysis under missing data, Comput. Struct. 182 (2017) 26–40.
[16] Y. Zhang, L. Comerford, I. Kougioumtzoglou, M. Beer, Lp-norm minimization for stochastic process power spectrum estimation subject to incomplete data, Mech. Syst. Signal Process. 101 (2017) 361–376.
[17] M.B. Priestley, Spectral Analysis and Time Series, Elsevier Academic Press, Amsterdam, 1996.
[18] D. Gabor, Theory of communication. Part 1: the analysis of information, J. Inst. Electr. Eng. - Part III: Radio Commun. Eng. (1946) 429–441.
[19] D. Gabor, Theory of communication. Part 2: the analysis of hearing, J. Inst. Electr. Eng. - Part III: Radio Commun. Eng. (1946) 442–445.
[20] D. Gabor, Theory of communication. Part 3: frequency compression and expansion, J. Inst. Electr. Eng. - Part III: Radio Commun. Eng. (1946) 445–457.
[21] J. Morlet, G. Arens, E. Fourgeau, D. Giard, Wave propagation and sampling theory; Part I, complex signal and scattering in multilayered media, Geophysics 47 (2) (1982) 203–221.
[22] J. Morlet, G. Arens, E. Fourgeau, D. Giard, Wave propagation and sampling theory; Part II, sampling theory and complex waves, Geophysics 47 (2) (1982) 222–236.
[23] D.E. Newland, Harmonic and musical wavelets, Proc. R. Soc. Lond. Ser. A: Math. Phys. Sci. 444 (1922) (1994) 605–620.
[24] D.E. Newland, Wavelet analysis of vibration: part 1—theory, J. Vib. Acoust. 116 (4) (1994) 409–416.
[25] D.E. Newland, Wavelet analysis of vibration: part 2—wavelet maps, J. Vib. Acoust. 116 (4) (1994) 417–425.
[26] P.D. Spanos, J. Tezcan, P. Tratskas, Stochastic processes evolutionary spectrum estimation via harmonic wavelets, Comput. Methods Appl. Mech. Eng. 194 (12–16) (2005) 1367–1383.
[27] P.D. Spanos, I.A. Kougioumtzoglou, Harmonic wavelets based statistical linearization for response evolutionary power spectrum determination, Probab. Eng. Mech. 27 (1) (2012) 57–68.
[28] I.A. Kougioumtzoglou, P.D. Spanos, Harmonic wavelets based response evolutionary power spectrum determination of linear and non-linear oscillators with fractional derivative elements, Int. J. Non Linear Mech. 80 (2016) 66–75.
[29] S.R. Massel, Wavelet analysis for processing of ocean surface wave records, Ocean Eng. 28 (8) (2001) 957–987.
[30] P.C. Liu, A.V. Babanin, Using wavelet spectrum analysis to resolve breaking events in the wind wave time series, Ann. Geophys. 22 (10) (2004) 3335–3345.
[31] A. Veltcheva, C. Guedes Soares, Wavelet analysis of non-stationary sea waves during Hurricane Camille, Ocean Eng. 95 (2015) 166–174.
[32] R. Prahlada, P.C. Deka, Forecasting of time series significant wave height using wavelet decomposed neural network, Aquat. Procedia 4 (2015) 540–547.
[33] S. Shahabi, M.-J. Khanjani, Modelling of significant wave height using wavelet transform and GMDH, in: Proceedings of the 36th IAHR World Congress, The Hague, The Netherlands, 2015.
[34] D.E. Newland, Ridge and phase identification in the frequency analysis of transient signals by harmonic wavelets, J. Vib. Acoust. 121 (2) (1999) 149–155.
[35] E.J. Candes, J. Romberg, T. Tao, Robust uncertainty principles: exact signal reconstruction from highly incomplete frequency information, IEEE Trans. Inf. Theor. 52 (2) (2006) 489–509.
[36] M.A. Davenport, M.F. Duarte, Y.C. Eldar, G. Kutyniok, Introduction to compressed sensing, in: Y.C. Eldar, G. Kutyniok (Eds.), Compressed Sensing: Theory and Applications, Cambridge University Press, Cambridge, UK, 2012, pp. 1–64.
[37] E.J. Candes, M.B. Wakin, An introduction to compressive sampling, IEEE Signal Process. Mag. 25 (2) (2008) 21–30.
[38] NOAA, Handbook of Automated Data Quality Control Checks and Procedures, National Data Buoy Center, Mississippi, USA, 2009.
[39] K. Hasselmann, T.P. Barnett, E. Bouws, H. Carlson, D.E. Cartwright, K. Eake, J.A. Euring, A. Gicnapp, D.E. Hasselmann, P. Kruseman, A. Meerburg, P. Mullen, D.J. Olbers, K. Richren, W. Sell, H. Walden, Measurements of wind-wave growth and swell decay during the joint North Sea wave project (JONSWAP), in: Ergänzungsheft zur Deutschen Hydrographischen Zeitschrift A8, 1973, pp. 1–95.
[40] W.J. Pierson, L. Moskowitz, A proposed spectral form for fully developed wind seas based on the similarity theory of S. A. Kitaigorodskii, J. Geophys. Res. 69 (24) (1964) 5181–5190.